*Structural Engineering and Mechanics, Vol. 35, No. 4 (2010) 459-478* 459
DOI: http://dx.doi.org/10.12989/sem.2010.35.4.459

# Modelling of seismically induced storey-drift in buildings

Nelson Lam[1]*, John Wilson[2] and Elisa Lumantarna[1]

[1]*Department of Civil & Environmental Engineering, University of Melbourne, Parkville, Victoria, Australia*
[2]*Faculty of Engineering and Industrial Science, Swinburne University of Technology, Hawthorn, Victoria, Australia*

*(Received February 7, 2009, Accepted February 11, 2010)*

**Abstract.** This paper contains detailed descriptions of a dynamic time-history modal analysis to calculate deflection, inter-storey drift and storey shear demand in single-storey and multi-storey buildings using an EXCEL spreadsheet. The developed *spreadsheets* can be used to obtain estimates of the dynamic response parameters with minimum input information, and is therefore ideal for supporting the conceptual design of tall building structures, or any other structures, in the early stages of the design process. No commercial packages, when customised, could compete with *spreadsheets* in terms of simplicity, portability, versatility and transparency. An innovative method for developing the stiffness matrix for the lateral load resistant elements in medium-rise and high-rise buildings is also introduced. The method involves minimal use of memory space and computational time, and yet allows for variations in the sectional properties of the lateral load resisting elements up the height of the building and the coupling of moment frames with structural walls by diaphragm action. Numerical examples are used throughout the paper to illustrate the development and use of the *spreadsheet* programs.

**Keywords:** seismic; storey drift; EXCEL; dynamic modal analysis; tall buildings.

## 1. Introduction

The earthquake resistant design of reinforced concrete and structural steel buildings has been well documented (e.g., Paulay and Priestley 1992, Priestley 1996, Krawinkler 1996). However, emphasis on cited publications have been on the design and detailing practices and the assessment of the strength and ductility capacity of the lateral resisting elements of the buildings, namely structural walls and moment resisting frames. Practical issues associated with the realistic modelling of the structure for simulating their dynamic response behaviour in an earthquake have only been addressed in more recent times (e.g., Elghazouli 2003, Kelly 2004, Cotsovos and Pavlovic 2006). Meanwhile, realistic modelling of the properties of the ground shaking which has incorporated effects of site amplification is equally critical (e.g., review articles by Lam *et al.* 2000, Lam *et al.* 2007, Chandler *et al.* 2002, Lam *et al.* 2001).

Different methods have been developed for estimating seismic actions in a building structure, namely the quasi-static analysis method and the dynamic analysis method which can be sub-divided

*Corresponding author, Ph.D., E-mail: ntkl@unimelb.edu.au

into the response spectrum analysis method and the time-history simulation method. Traditionally, quasi-static analysis method is favoured by structural engineering designers for reasons of simplicity. Effects of the higher modes of vibration (which are not automatically accounted for by the quasi-static model) have been emulated by the application of fictitious forces applied at the upper level of the building, and/or by artificially increasing response spectral accelerations in the high period range.

Whilst a quasi-static model is easy to comprehend and use, the proliferated access to computers and the advent of commercial packages with dynamic analysis capabilities have increased the use of dynamic analyses in the design of new building structures and the assessment of existing structures. Most international seismic codes of practice make dynamic analysis a mandatory requirement for tall buildings. For example, the Australian Standard for Structural Actions: Seismic Actions (AS1170.4 2007) requires buildings that are taller than 50 m to be assessed using a dynamic analysis.

Dynamic analysis of building models comprising beam and column elements or finite elements can be implemented using well known commercial packages such as *ABACUS*, *ANSYS*, *Strand* and *SPACEGASS*. However, analysis of this nature can only be undertaken at the later stage of the detailed design of the building when details of the configuration of the structural elements and their dimensions are known. Information on the quantities of longitudinal reinforcement and the axial load ratio in a reinforced concrete member that is dominated by flexural actions will also be required for the accurate calculation of the post-cracked stiffnesses. Thus, the effective stiffness of a reinforced concrete member cannot always be generalised as a fraction of the initial (uncracked) stiffness. References are made to the work by Priestley *et al.* (2007), Priestley (1998), Priestley and Kowalsky (1998), Numayr *et al.* (2003) and Yun *et al.* (2004) which cover the behaviour of both normal strength and high strength concrete. Finite element analyses that have not incorporated such details will result in significant errors. Clearly, there are difficulties in implementing a finite element dynamic analysis in the early stages of the design of the building structure.

A more effective alternative method is to employ simplified models, such as macro models, for simulating the potential seismic response behaviour of the building structure throughout the design process. Macro models of reinforced concrete have evolved in different forms. For example, a macro model of a concrete member can be a finite model which has a relatively smaller number of elements in order to save memory space and computational time whilst aiming at simulating the global deflection behaviour of the member (e.g., Kelly 2004, Qian and Chen 2005). Macro models have also been used for analysing the out-of-plane response behaviour of unreinforced masonry walls (e.g., Lam *et al.* 1995, 2004) and the overturning of objects in buildings (e.g., Al Abadi *et al.* 2004, 2006). Simplified macro model of a building could also be developed from information inferred from the structural floor plans. Thus, *macro* modelling can be undertaken as early as the conceptual design stage.

Numerous *macro* models have been developed for obtaining estimates of the inter-storey drift demand of multi-storey buildings. These *macro* models are vertical elements to represent contributions by the moment resisting frames and shear walls to the lateral resistance of the building. Models developed by Iwan (1997) and Gulkan and Akkar (2002) were of the form of simple shear beams in which flexural actions of the shear walls have not been included. A more elaborate model based on the joint contributions of a shear beam element (representing moment resisting frames) and a vertical cantilever element (representing shear walls) have been developed by Miranda (1999). The model was further developed by Miranda and Reyes (2002) to incorporate allowances for variation in the lateral stiffness of the element up the height of the building. Importantly, inter-storey drift demands as predicted by these *macro* models for low and medium rise buildings (which are dominated by the fundamental mode of vibration) have been demonstrated to be in good agreement with results from time-history analysis of the finite element model of the building. However, significant discrepancies have been found with high period (tall) buildings in certain conditions given that these simplified methods of analysis were typically based on a pre-determined horizontal load profile which cannot fully represent higher mode actions in the building. Higher mode effects have been accurately accounted for in a more recently developed calculation procedure presented by Miranda and Akkar (2006).

The *macro* model introduced in this paper operates with similar principles but possesses the unique feature of allowing the variation of mass and stiffness up the height of the building to be specified arbitrarily (which is in contrasts to the generalization approach adopted by a typical *macro* model presented in the literature). This is accomplished by the use of matrix approach in operating Virtual Work Method for finding deflections conveniently (exploiting the capability of spreadsheets). This calculation approach is distinct from the classical approach of solving 4th order differential equations for finding deflections as done in the development of many *macro* models described above. A key feature of the presented methodology is the instantaneous calculation and display of the modal properties and time-histories of selected response quantities (e.g., inter-storey drifts and base shear). Thus, higher mode effects have also been taken into account systematically. The use of spreadsheets and *macro* models for dynamic simulations enables seismic actions in the structure to be assessed conveniently and with much less time and effort. The low cost feature of the simulations allows sensitivity studies to be undertaken in order that the potential implications of different schematic designs can be anticipated and evaluated using preliminary information. It is acknowledged that such capabilities can be achieved with a commercial package by customising the input interface of the program, but, no customisation could compete with spreadsheets in terms of simplicity, portability, versatility and transparency. Transparency is an important attribute of the proposed calculation approach given that the blackbox syndrome is particularly an issue with dynamic simulations where engineers often find it difficult to cross-check simulations from simple hand calculations.

The algorithms presented in this paper are restricted to analyses for linear elastic behaviour. By the traditional *Equal Displacement* proposition, the inelastic displacement demand of a single-degree-of-freedom system may be assumed to be equal to the calculated displacement demand based on linear elastic behaviour and 5% damping. This simple estimate of the displacement demand would need to be modified to reconcile with results observed from non-linear time-history analyses in certain conditions. The modification factor has been found to be dependent on the natural period of the building, the dominant period of the applied excitations and the displacement ductility level as revealed by numerous studies including the well known studies undertaken by Miranda (1991, 1993, 1999). For a building dominated by the fundamental mode of vibration, the application of the modification in the spreadsheet calculation is straightforward: the elastic spectral displacement (for 5% damping) is simply amplified by the modification factor (proposed by publications cited above) and the amplified value is then used to combine with the participation factor and the mode shape vector for the calculation of the storey drift demands. Conversely, the strength demand obtained from a linear elastic analysis could be scaled down by the strength reduction factor (which is also known as the structural response modification factor or behaviour factor) to allow for the beneficial effects of the ductile response behaviour of the structure. Readers may refer to Miranda and Ruiz-Garcia (2002) in which a range of proposed reduction factor models have been reviewed. For buildings in which higher mode effects are significant, only the strength demand associated with the fundamental mode of vibration is scaled down whilst contributions by the higher modes should be taken as the original value as obtained from linear elastic analysis which is contrary to most contemporary code provisions (Priestley *et al.* 2007).

In view of the well established guidelines that have been provided by the literature on the use of modification factors to allow for inelastic behaviour, the rest of the paper put the focus on dynamic response calculations based on linearly elastic behaviour and the techniques of automating those calculations on spreadsheets.

The remainder of the paper is divided into Sections 2, 3 and 4. In Section 2, the *spreadsheet* implementation of the simulations of the seismically induced drift behaviour of single-degree-of-freedom systems including that of single-storey buildings is illustrated (Fig. 1(a)). In Section 3, the simulation methodology is extended to the analysis of a 3-storey building which is represented by a *macro* model (Fig. 1(b)). In Section 4, an innovative method using *spreadsheets* for constructing the stiffness matrix for the lateral load resistant elements of taller buildings is introduced. The method involves minimal use of memory space and computation time, and yet allows for variations in the sectional properties of the lateral load resisting elements up the height of the building together with the coupling of moment frames with structural walls by diaphragm action (Fig. 1(c)). The modal natural periods and mode shapes computed by *spreadsheets* for an example 10-storeys building will

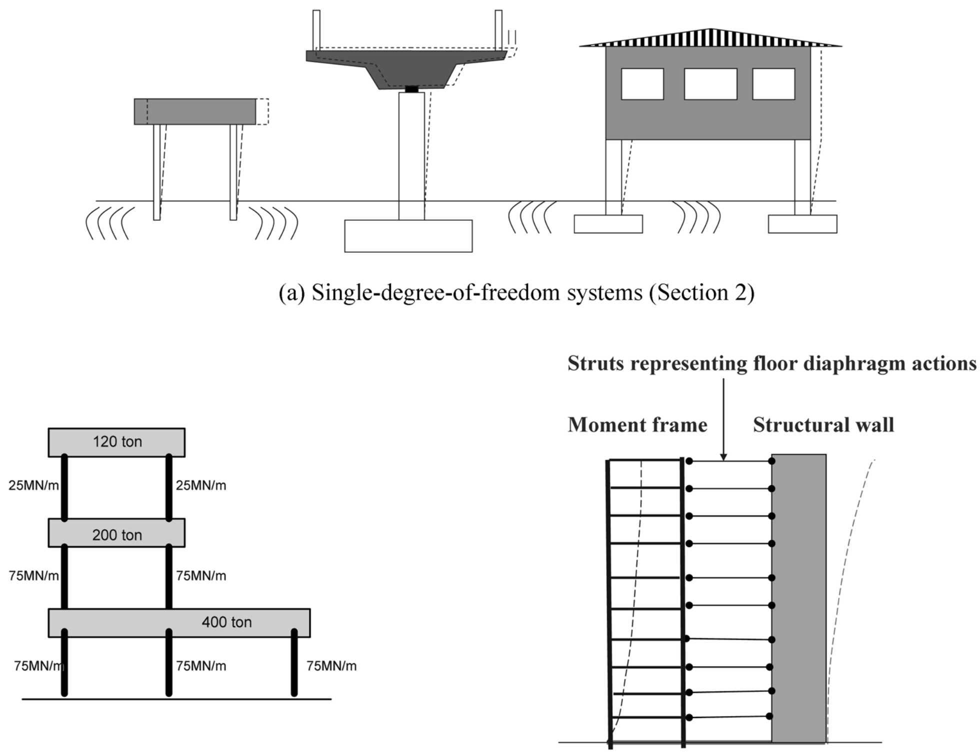


(a) Single-degree-of-freedom systems (Section 2)

(b) 3-storeys building (Section 3)

(c) 10-storeys building (Section 4)

Fig. 1 Example structures included in the illustrations be compared with those obtained from a commercial computer package.

Since the originality of the paper is in the implementation of the computations by *spreadsheets*, relationships that are based on established principles have been summarised as background notes in particular figures, rather in the main text (whereas detailed descriptions of the relevant concepts can be found in standard structural dynamics text books such as Chopra (2000)).

## 2. Time-history simulations for single-storey buildings

### 2.1 Time-step integration methods

The common methods for simulating the response time-histories for single-degree-of-freedom systems are namely the *Duhamel Integration Method* and *Time-step Integration Methods*. The *Duhamel Integration Method* (based on solving the convolution integral) can occupy a great deal of memory and requires lengthy computational time for irregular and sustained excitations such as that generated by an earthquake (a large number of *Dirac-Delta* functions are required to simulate the response of every pulse in the excitation). Time-step Integration is about predicting the displacement, velocity and acceleration of the next time step using those quantities calculated in the previous two time-steps. Computation begins with the first time-step at which the initial conditions are defined. Time-step Integration can be very efficient and accurate if the time-step interval is sufficiently short, and can be readily extended to solving the response of non-linear systems, unlike the *Duhamel Integration Method* which is restricted to solving the response of linear elastic systems only.

Time-step Integration Methods can be sub-classified into : (i) *Central Difference Method* (which is simple to operate in the spreadsheet but is less accurate), (ii) *Constant Average Acceleration Method* (which is unconditionally stable and hence most suited to be used for the solution of matrices representing systems possessing large numbers of degrees of freedom), (iii) *Linear Average Acceleration Method* (which is amongst the most accurate of all the methods but not as stable as the *Constant Average Acceleration Method)*, and (iv*) Wilson $\theta$ Method* (which was modified from the *Linear Average Acceleration Method*; with a value of $q$ = 1.42 recommended for optimal accuracy).

The remainder of this section illustrates the *spreadsheet* implementation of the *Central Difference Method* for solving the displacement time-history of single-degree-of-freedom systems in response to ground excitations.

### 2.2 Central difference method

Relationships associated with the *Central Difference Methods* are summarised in Fig. 2(a) for background information. The overall strategy of the operation is to find displacement at time step $j+1$ given the displacement at the two previous time steps: $j$ and $j-1$. An example implementation of the spreadsheet method is illustrated in Fig. 2(b). For detailed descriptions of the method and the listed relationships, consult standard structural dynamic textbooks such as Chopra (2000).

It is noted that with *Central Difference Method*, the solution can become unstable if $\Delta t \geq T/\pi$. For example, numerical instability resulting in gross errors can occur if the time-step $\Delta t \geq 0.03$ sec in the analysis of a *SDOF* system with $T$ = 0.1 sec. Furthermore, $\Delta t$ should be made as small as possible, and preferably $\Delta t \leq T/10$ for accurate results.

$$\dot{u}_j = \frac{u_{j+1} - u_{j-1}}{2\Delta t}$$

By similar reasoning:

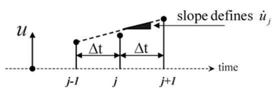


$$\ddot{u}_j = \frac{\dot{u}_{j+\frac{1}{2}} - \dot{u}_{j-\frac{1}{2}}}{\Delta t} = \frac{\left(\frac{u_{j+1} - u_j}{\Delta t}\right) - \left(\frac{u_j - u_{j-1}}{\Delta t}\right)}{\Delta t} = \frac{u_{j+1} - 2u_j + u_{j-1}}{\Delta t^2}$$

$$\ddot{u}_j + 2\xi\omega_n\dot{u}_j + \omega_n^2 u_j = \frac{p(t)}{m} \text{ or } -\ddot{u}_{gj} \Rightarrow$$

$$u_{j+1} = \frac{-\ddot{u}_{gj} + \underbrace{\left(-\omega_n^2 + \frac{2}{\Delta t^2}\right)}_{A} u_j + \underbrace{\left(\frac{\xi\omega_n}{\Delta t} - \frac{1}{\Delta t^2}\right)}_{B} u_{j-1}}{\underbrace{\frac{1}{\Delta t^2} + \frac{\xi\omega_n}{\Delta t}}_{C}}$$

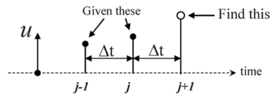


Fig. 2(a) Background to the *Central Difference Method*

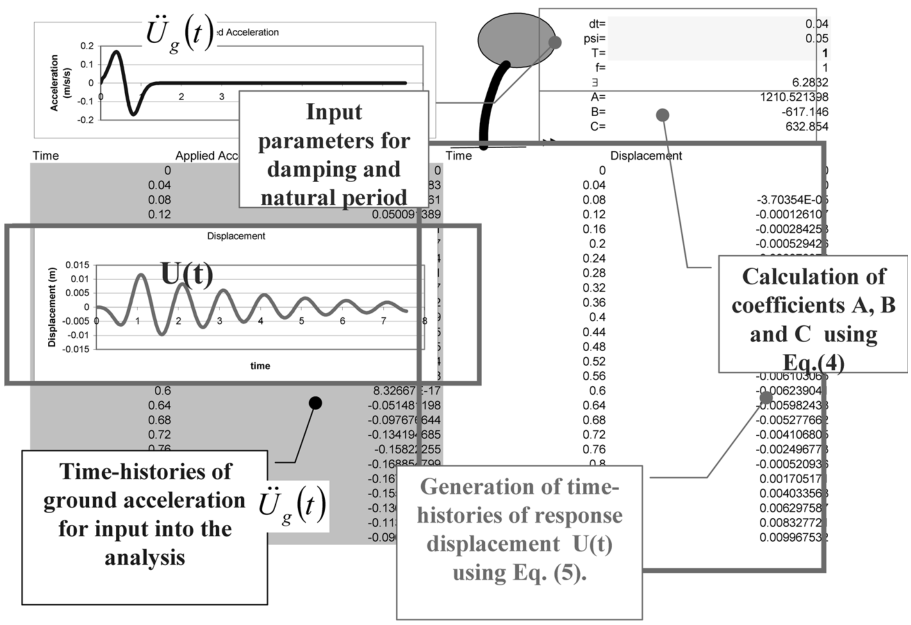


Fig. 2(b) Implementation of *Central Difference Method* in a *spreadsheet*

### *2.3 Illustration by example*

The "*Newhall-1*" accelerogram recorded during the 1994 Northridge Earthquake was chosen to generate the response time-history of a linear elastic (1-second period) single-degree-of-freedom system with 5% damping using the developed spreadsheet. Figs. 3(a) and 3(b) present the time-histories of the (input) acceleration of the ground, $\ddot{U}_g(t)$ and the (output) response displacement of the lumped mass system, $U(t)$ respectively.

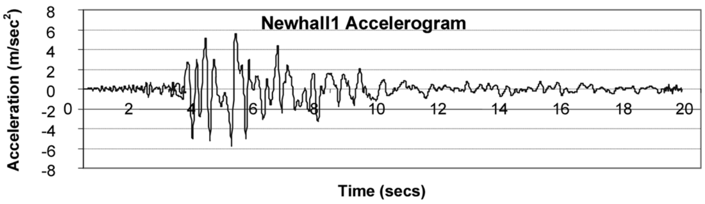


(a) Acceleration time-history of the ground (input)

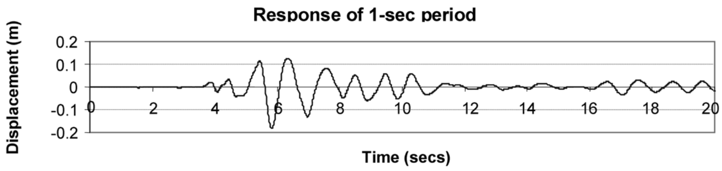


(b) Response displacement time-history of system (output)

Fig. 3 Input and Output time-histories of analysis by *Central Difference Method*

## 3. Modal analyses and time-history simulations for 3-storey buildings

### 3.1 Mode shape iteration method

The eigenvalue of a two or three degree-of-freedom (*2DOF* or *3DOF*) system can be obtained by solving the roots of a polynomial expression based on equating the determinant of the matrix: $Det\|[K]-\lambda[M]\|$ to zero. This elementary approach of obtaining eigensolutions would not be feasible for systems with a large number of *DOF's*. The mode shape iteration method (which is also known as the Power Method) is considered more viable for dealing with systems with much larger *DOF's.* The basic principles used in developing the mode shape iteration method and the associated relationships are summarised in Figs. 4(a), (b) as background information.

Let $[K]$ = stiffness matrix; $[M]$ = mass matrix;
$\{U\}$ = displacement vector; $\lambda$ = eigenvalue; and $\{\phi\}$ = mode shape vector

$$\text{Given that}: [K]\{U\}=\lambda[M]\{U\} \quad \text{or} [K]\{\phi\}=\lambda[M]\{\phi\}$$

Let flexibility matrix $[F]=[K]^{-1}$
Pre-multiply both sides of the equation by $[F]$:

$$[F][K]\{\phi\}=\lambda[F][M]\{\phi\} \Rightarrow \{\phi\}=\lambda[F][M]\{\phi\}$$

Let $[D]=[F][M]$:

$$\{\phi\}=\lambda[D]\{\phi\}$$

(a) Key relationships

Fig. 4 Background to the *Mode Shape Iteration Method*

Given that: $\{\phi\} = \lambda[D]\{\phi\}$

In the initial (zeroth) iteration, let $\lambda_0 = 1$ and $\{\phi\}_0 \Rightarrow \begin{Bmatrix} 1 \\ 1 \\ 1 \end{Bmatrix}$

$$\{\phi\}_1 = [D]\{\phi\}_0 \quad \lambda_1 = \frac{\{\phi\}_1^T[K]\{\phi\}_1}{\{\phi\}_1^T[M]\{\phi\}_1}$$

normalisation : $\{\hat{\phi}\}_1 = \dfrac{\{\phi\}_1}{\sqrt{\{\phi\}_1^T[M]\{\phi\}_1}}$; take $\{\phi\}_1 = \{\hat{\phi}\}_1$ for next iteration

$$\{\phi\}_2 = [D]\{\phi\}_1 \quad \lambda_2 = \frac{\{\phi\}_2^T[K]\{\phi\}_2}{\{\phi\}_2^T[M]\{\phi\}_2}$$

normalisation : $\{\hat{\phi}\}_2 = \dfrac{\{\phi\}_2}{\sqrt{\{\phi\}_2^T[M]\{\phi\}_2}}$; take $\{\phi\}_2 = \{\hat{\phi}\}_2$ for next iteration

and so on .........

$$\{\phi\}_i = [D]\{\phi\}_{i-1} \quad \lambda_i = \frac{\{\phi\}_i^T[K]\{\phi\}_i}{\{\phi\}_i^T[M]\{\phi\}_i}$$

normalisation : $\{\hat{\phi}\}_i = \dfrac{\{\phi\}_i}{\sqrt{\{\phi\}_i^T[M]\{\phi\}_i}}$. Iteration stops as $\{\phi\}_i$ and $\lambda_i$ converge

(b) Iteration and normalisation of eigenvector

Fig. 4 Background to the *Mode Shape Iteration Method* (continued)

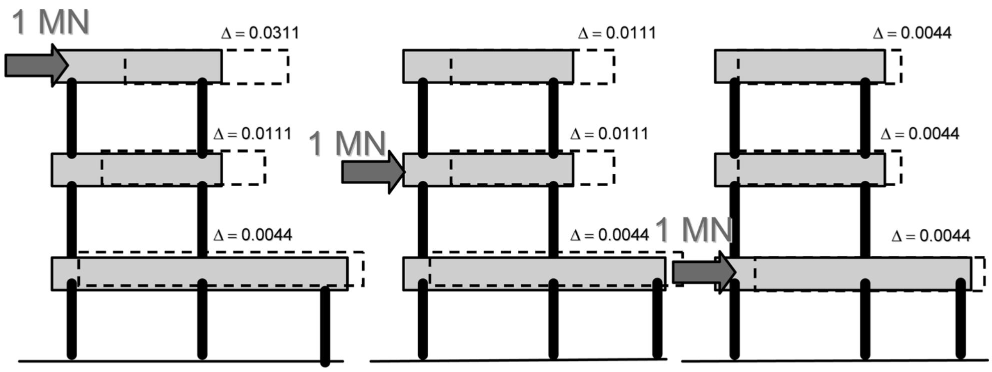


Fig. 5 Unit load analyses for determination of [*F*] matrix

### *3.2 Illustration by example*

The method is illustrated by the analytical case study of an example building with storey mass and storey stiffness as defined in Fig. 1(b). A unit horizontal force is applied at each and every storey level to derive the flexibility matrix of the frame as shown in Fig. 5. The Flexibility Matrix can be constructed with the displacement values obtained from the unit load analyses and inverted to obtain the stiffness matrix. The Mass Matrix and the *D* matrix are identified accordingly as illustrated in Eqs. (1a)-(1d).

$$\text{Flexibility matrix } [F] = \begin{bmatrix} 31 & 11 & 4.4 \\ 11 & 11 & 4.4 \\ 4.4 & 4.4 & 4.4 \end{bmatrix} \quad \text{units in m/MN} \times 10^{-3} \tag{1a}$$

$$\text{Stiffness matrix [K]} = \begin{bmatrix} 50 & -50 & 0 \\ -50 & 200 & -150 \\ 0 & -150 & 377 \end{bmatrix} \quad \text{units in MN/m} \tag{1b}$$

$$\text{Mass matrix [M]} = \begin{bmatrix} 120 & 0 & 0 \\ 0 & 200 & 0 \\ 0 & 0 & 400 \end{bmatrix} \times 10^{-3} \quad \text{units in kilo-tonnes} \tag{1c}$$

$$[D] = [F][M] = \begin{bmatrix} 31 & 11 & 4.4 \\ 11 & 11 & 4.4 \\ 4.4 & 4.4 & 4.4 \end{bmatrix} \begin{bmatrix} 120 & 0 & 0 \\ 0 & 200 & 0 \\ 0 & 0 & 400 \end{bmatrix} \times 10^{-6} = \begin{bmatrix} 3.73 & 2.21 & 1.76 \\ 1.33 & 2.21 & 1.76 \\ 0.53 & 0.88 & 1.76 \end{bmatrix} \times 10^{-3} \tag{1d}$$

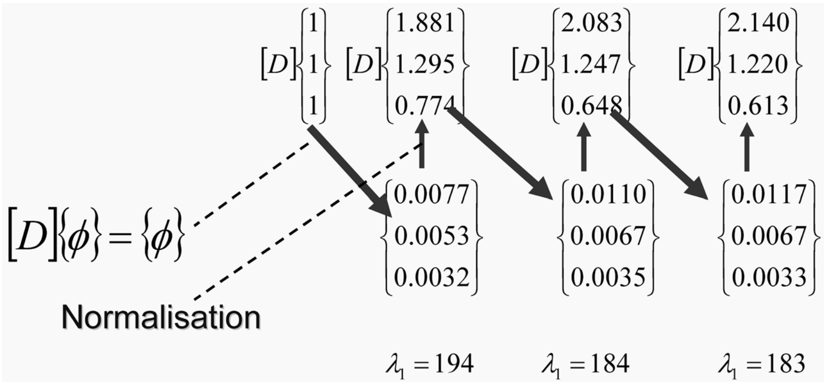


Fig. 6 Spreadsheet operations for the calculation of the 1st mode of natural vibration

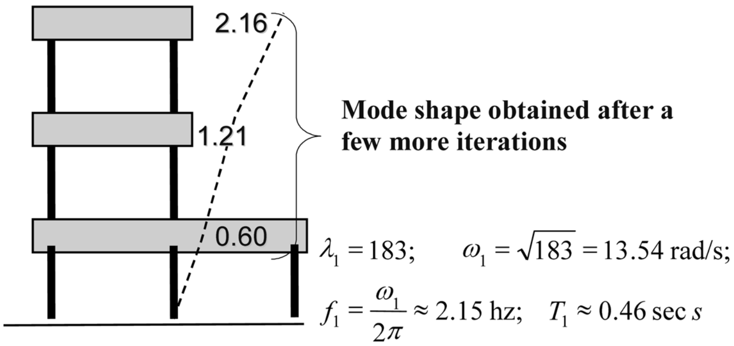


Fig. 7 Eigensolution for the 1st mode of natural vibration

The mode shape iteration method can then be applied to calculate the first eigenvalue ($\lambda$) and eigenvector ($\phi$) using the [$D$] matrix as summarised in Fig. 6 whilst the eigenvalue solution obtained for the first mode of vibration is shown in Fig. 7.

The computation procedure illustrated in the above only provides solutions for the 1st (fundamental) mode of natural vibration. The calculation technique for obtaining the 2nd and higher modes of natural vibration involves applying a "shift" ($\mu$) to the eigenvalue; i.e., $\lambda = \lambda' + \mu$. The original expression: $[K]\{\phi\} = \lambda[M]\{\phi\}$ becomes $[K]\{\phi\} = (\lambda' + \mu)[M]$ which is then translated into: $[[K] - \mu[M]]\ \{\phi\} = \lambda'[M]$. The value of $\lambda'$ is then found by iteration in the manner as described in Fig. 4(a), but the relationship to be used is : $\{\phi\} = \lambda'[D]'\{\phi\}$ where $[D]'$ is derived from the transformed stiffness matrix: $[[K] - \mu[M]]$. In a trial and error procedure, the value of $\mu$ is incremented until the mode shape vector switch abruptly from that of the 1st natural vibration mode to the 2nd natural vibration mode. The value of $\mu$ is then incremented further until the mode shape vector switches again from that of the 2nd natural vibration mode to the 3rd natural vibration mode, and so on. Detailed description of this technique can be found in Chopra (2000). In the example calculation shown below, a shift of $\mu = 700$ is applied to obtain the eigensolution for the 2nd mode of vibration.

$$[k]' = [k] - \mu[M] = [k] - 700[M] = \begin{bmatrix} 50-700(0.12) & -50 & 0 \\ -50 & 200-700(0.2) & -150 \\ 0 & -150 & 377-700(0.4) \end{bmatrix} \tag{2a}$$

$$[k]' = \begin{bmatrix} -34 & -50 & 0 \\ -50 & 60 & -150 \\ 0 & -150 & 97 \end{bmatrix}; \quad [F]' = \begin{bmatrix} -51 & 15 & 23 \\ 15 & -10 & -16 \\ 23 & -16 & -14 \end{bmatrix} \times 10^{-3}$$

$$[D]' = [F]'[M] = \begin{bmatrix} -51 & 15 & 23 \\ 15 & -10 & -16 \\ 23 & -16 & -14 \end{bmatrix} \begin{bmatrix} 120 & 0 & 0 \\ 0 & 200 & 0 \\ 0 & 0 & 400 \end{bmatrix} \times 10^{-6} = \begin{bmatrix} -6.17 & 2.99 & 9.2 \\ 1.79 & -2.03 & -6.3 \\ 2.77 & -3.14 & -5.6 \end{bmatrix} \times 10^{-3} \tag{2b}$$

The mode shape iteration method is then applied once again for the calculation of the eigenvalue ($\lambda'$) and the eigenvector ($\phi$) for the 2nd mode of natural vibration using the [$D$]' matrix which is based on a shift value of $\mu = 700$. Details of the calculations are illustrated in Figs. 8 and 9.

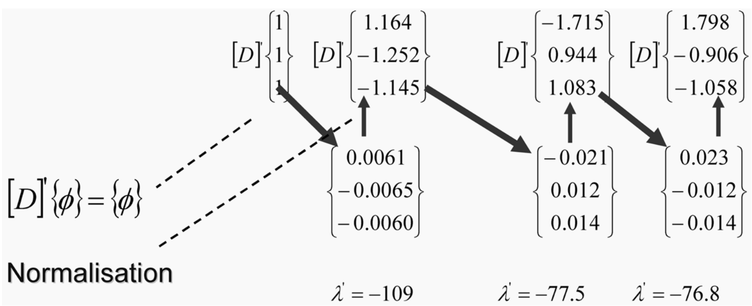


Fig. 8 Shaded box showing spreadsheet operations for the calculation of the 2nd mode of natural vibration

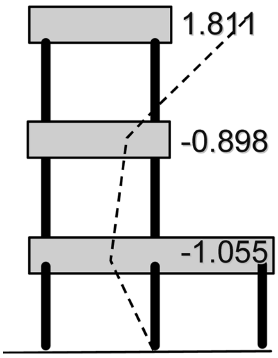


$$\lambda' = -76.8; \quad \mu = 700; \quad \lambda' = \lambda - \mu \Rightarrow$$

$$\lambda = \lambda' + \mu$$

Knowing that it is the 2nd mode of vibration.

Then, let $\lambda_2 = \lambda' + \mu \Rightarrow$

$$\lambda_2 = -76.8 + 700 = 623; \quad \omega_2 = \sqrt{623} = 25 \text{ rad/s};$$

$$f_2 = \frac{\omega_2}{2\pi} \approx 3.97 \text{ hz}; \quad T_2 \approx 0.25 \text{ sec}$$

Fig. 9 Eigensolution for the 2nd mode of natural vibration

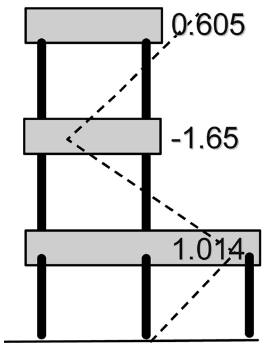


$$\lambda' = 53; \quad \mu = 1500; \quad \lambda' = \lambda - \mu \Rightarrow$$

$$\lambda = \lambda' + \mu$$

Knowing that it is the 3rd mode of vibration,

Then, let $\lambda_3 = \lambda' + \mu \Rightarrow$

$$\lambda_3 = 53 + 1500 = 1553; \quad \omega_3 = \sqrt{1553} = 39.4 \text{ rad/s};$$

$$f_3 = \frac{\omega_3}{2\pi} \approx 6.27 \text{ hz}; \quad T_2 \approx 0.16 \text{ sec}$$

Fig. 10 Eigensolution for the 3rd mode of natural vibration

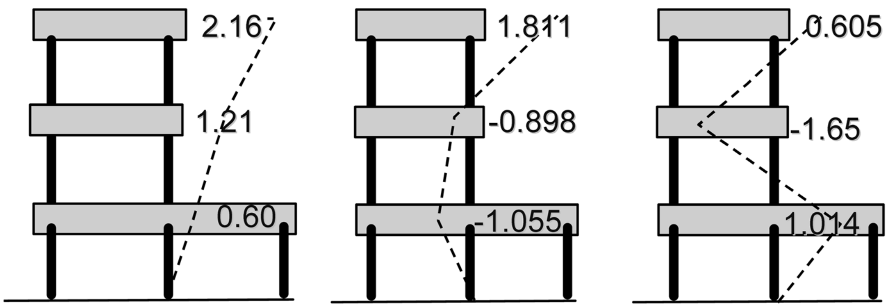


***$f_1$=2.15 hz; $T_1$=0.46sec*** ***$f_2$=3.97 hz; $T_2$=0.25sec*** ***$f_3$=6.27 hz; $T_3$=0.16sec***

Fig. 11 Summary of all eigensolutions

A further shift of $\mu$ = 1500 is then applied for calculation of the eigenvalue ($\lambda$) and the eigenvector ($\phi$) for the 3rd mode of natural vibration as shown in Fig. 10. The eigensolutions obtained for all three vibration modes are summarised in Fig. 11.

### 3.3 Simulation of the time-histories of the modal responses

The expressions listed in Fig. 12 are for estimating the displacement time-history of the building floor attributed to the $j$th mode of vibration using modal analysis theory where $U(t)$ is the displacement response time-history of a *SDOF* system (which has natural period equal to the modal period of vibration of the *MDOF* system), $\phi_{1,j}$ is the 1st entry (corresponding to node no. 1, the roof) to the mode shape vector $\{\phi\}_j$ for mode $j$, and $L_j/M_j$ is the participation factor for mode $j$. Given the modal storey displacements, the amount of modal inter-storey drift can be calculated by taking the difference in the displacement demand calculated for the adjacent stories. In the case

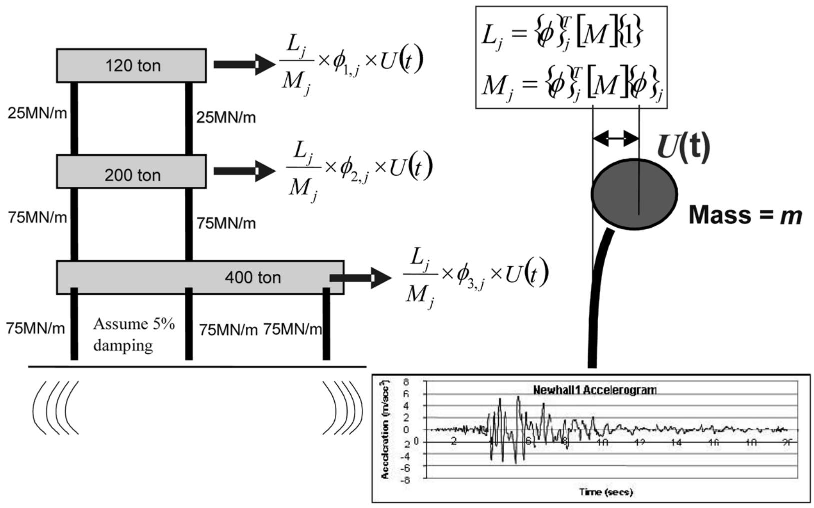


Fig. 12 Estimation of the modal displacement time-histories of the building floors

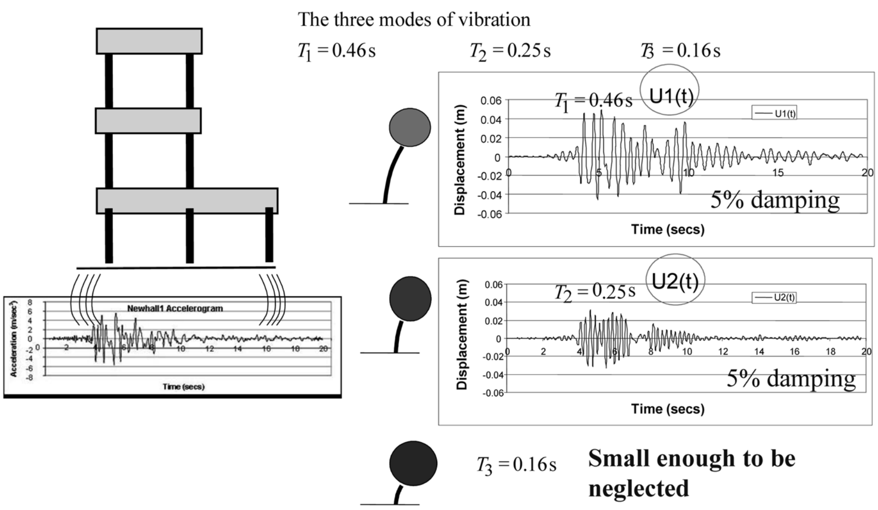


Fig. 13 Response time-histories of respective SDOF systems

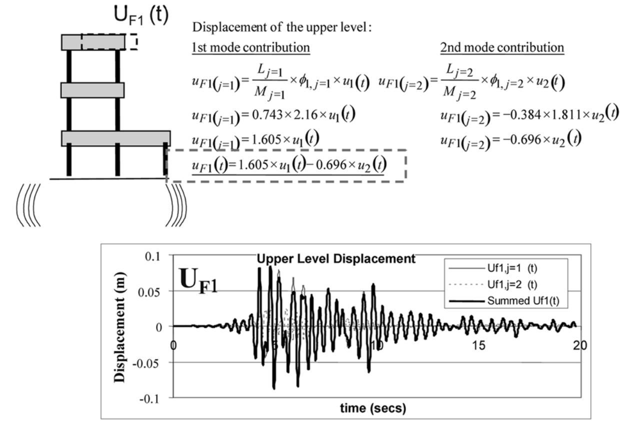


(a) Displacement at upper floor level

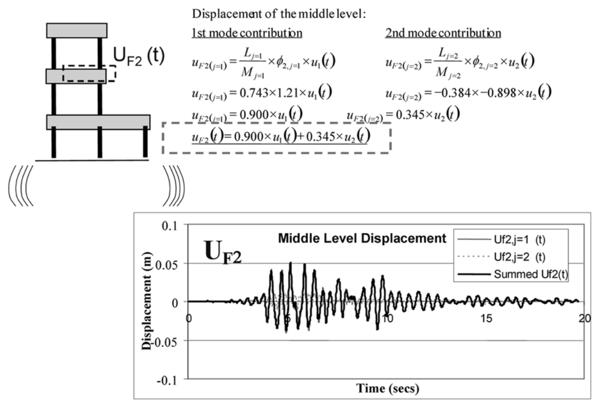


(b) Displacement at 2nd floor level

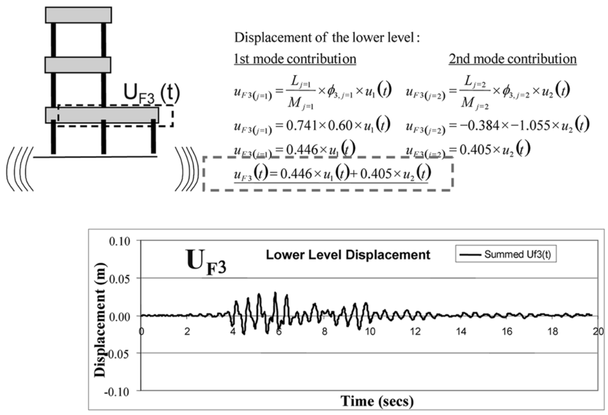


(c) Displacement at 1st floor level

Fig. 14 Storey displacement simulations

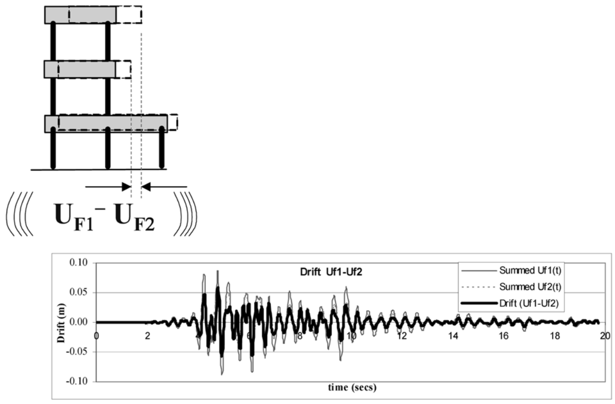


(a) Inter-storey drift at 2nd-3rd floor levels

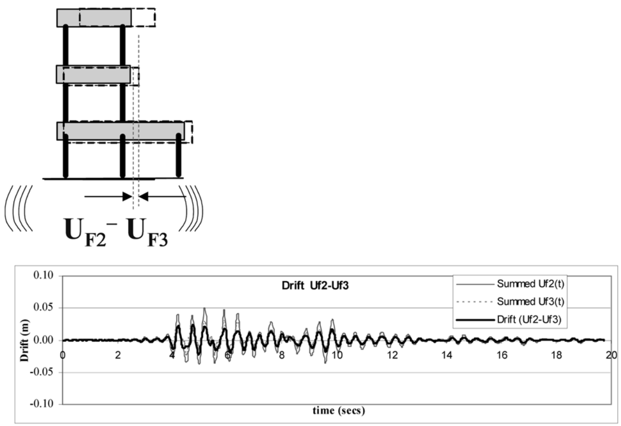


(b) Inter-storey drift at 1st-2nd floor levels

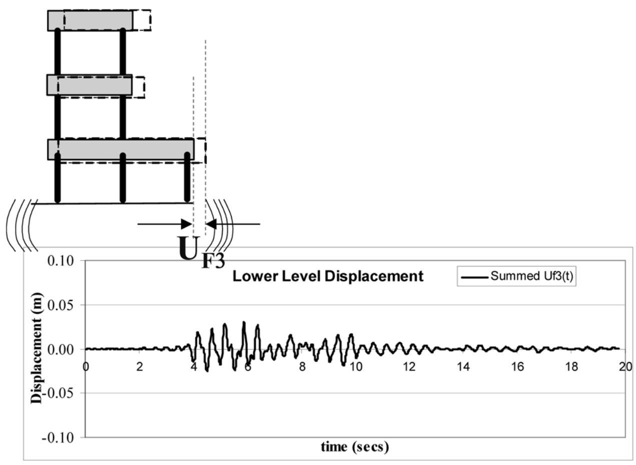


(c) Inter-storey drift at 1st floor level

Fig. 15 Inter-storey drift simulations

Table 1 Inter-storey shear forces of case study building

| Storey levels | Interstorey shear forces |
|---|---|
| Columns between 2nd and 3rd storey | 2950 kN |
| Columns between 1st and 2nd storey | 3650 kN |
| Columns between ground floor and 1st storey | 6850 kN |

study example to be illustrated in the remainder of this section, the analyses were based on the *Newhall*-1 accelerogram which was recorded from the 1994 Northridge earthquake (identical to the accelerogram used for simulations in Section 2).

The response time-histories simulated for SDOF systems with natural periods consistent with the modal periods of vibration have been calculated and are shown in Fig. 13.

The displacement at each individual storey levels attributed to the 1st and 2nd mode of vibrations have been simulated (Figs. 14(a)-14(c)). The amount of inter-storey drift have been calculated by taking the difference in storey displacements at each time step (Figs. 15(a)-15(c)). The maximum inter-storey shear forces have also been calculated as the product of the maximum inter-storey drifts and the storey stiffness (Table 1). It is noted that the presented inter-storey drifts and shear forces have already taken into account the combination of the first two modes of vibration at every time-step. This approach to modal combination is more accurate than the well known modal combination rules (such as the square-root-of-the-sum-of-the-squares method). It is noted that the sum of the interstorey shear forces (shown in Table 1) are not necessarily in equilibrium as they occur at different instances during the response of the building to the earthquake.

## 4. Modal analyses of taller buildings

### *4.1 Construction of flexibility, stiffness and dynamic Matrices*

In this section, the spreadsheet implementation of the construction of the flexibility matrices [$F$] and stiffness matrices [$K$] of tall buildings that are laterally supported by structural walls, moment frames or a dual system combining the contributions from the two types of elements are described. Fig. 16 is a schematic diagram of such a dual system which can be analysed by spreadsheet using the innovative technique described below.

The approach adopted herein is to build the flexibility matrix for the structural walls and moment frames in separate operations. The respective stiffness matrices are then obtained by matrix inversion which can be operated conveniently using spreadsheets for matrices representing tens of degrees-of-freedom (which will suffice for a *2D macro* modelling of a building). Separate flexibility matrices may be required to represent both the flexural and shear deflections of the lateral resisting element. An example of this is the case of a squat structural wall in which shear deflections of the wall can be as significant as the flexural deflections. Another example is a moment frame experiencing significant “push-pull” actions which can result in the overall curving of the frame in the direction of loading. The “flexural” deflection of the frame associated directly with the overall in-plane curvature can be as significant as the “storey-shear” of the frame which is associated directly with the deflection of the individual columns which bend in reversed curvature in between

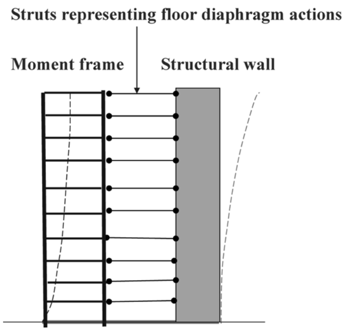


Fig. 16 Dual system of wall-frame

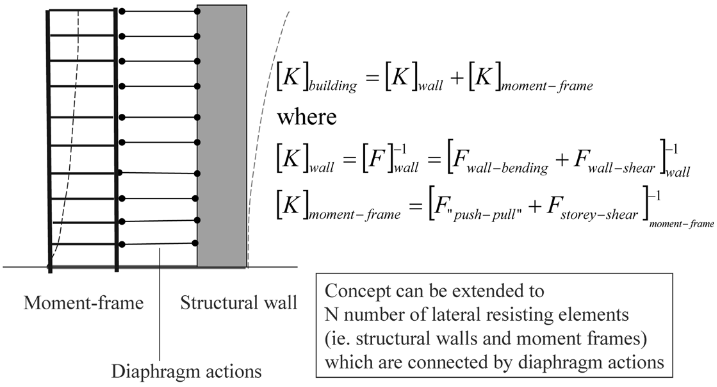


Fig. 17 Formulation of stiffness matrix

the floors (Accurate estimates of the “push-pull” actions are particularly important with tall moment frames supported by out-riggers.). The flexibility matrices representing different modes of deflections of walls, or frames (with or without out-riggers), can be summed to obtain the resultant flexibiltiy matrix in which all deflection components have been incorporated. The stiffness matrix of a lateral resisting element is then obtained by the matrix inversion of the resultant flexibility matrix.

The global stiffness matrix for the building is then obtained as the sum of the stiffness matrices of the individual lateral load resisting elements. This approach of assembling stiffness matrices enables dual systems of wall and frames to be obtained simply as the sum of the stiffness matrices of the wall and frame in isolation. The method of constructing the flexibility and stiffness matrices for a tall building is summarised in Fig. 17. The implicit assumption with this method of calculation is that the two types of systems are connected by diaphragm actions of the floor and there are no moment coupling between the systems. The dynamic matrix [*D*] can be obtained as the product of [*F*] and the diagonal Mass Matrix [*M*] in which only the translational inertia of the building floors have been taken into account.

The flexibility matrix [*F*] for representing the bending of a structural wall can be constructed by calculating the deflections at various levels up the height of the wall when subject to a horizontal force of unit magnitude (and applied one at a time at each reference level). Fig. 18(a) illustrates the use of the virtual force method in calculating the deflection of the wall at two-thirds the total height when subject to a unit force applied at the top of the wall. It is illustrated further in Fig. 18(b) that this calculation can be implemented in *spreadsheets* by the multiplication of a row vector with a column vector. By applying different values of *EI* to the “upper”, “middle” and “lower” segments of the column vector (as shown in Fig. 18(b)) variations in the sectional properties of the wall up the height of the building can be incorporated into the calculations. Importantly, the idea of multiplying a row vector with a column vector (for calculating the deflection at a reference point on the wall) has been extended into the idea of multiplying two matrices (for calculating entries to the flexibility matrix of the wall) as shown in Fig. 18(c).

The flexibility matrix for estimating shear deflections of a squat wall, or the equivalent shear stiffness of a moment-frame, can be constructed in a similar manner. In the calculation for shear deflections, the bending moment diagrams as illustrated in Figs. 18(a)-18(c) need to be replaced with shear force diagrams; and “*M/EI*” replaced with “*V/GA*” where *V* is the shear force, *G* is the

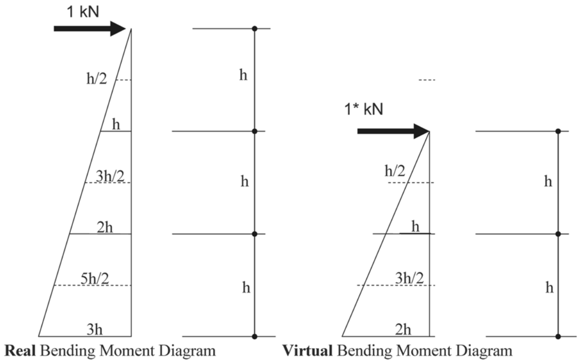


$$\Delta = \frac{h/2}{3EI}\left[\left\{h(0^*)+4\left(\frac{3h}{2}\right)\left(\frac{h^*}{2}\right)+2h(h^*)\right\}+\left\{2h(h^*)+4\left(\frac{5h}{2}\right)\left(\frac{3h^*}{2}\right)+3h(2h^*)\right\}\right]$$

(a) Calculation of deflection due to unit force

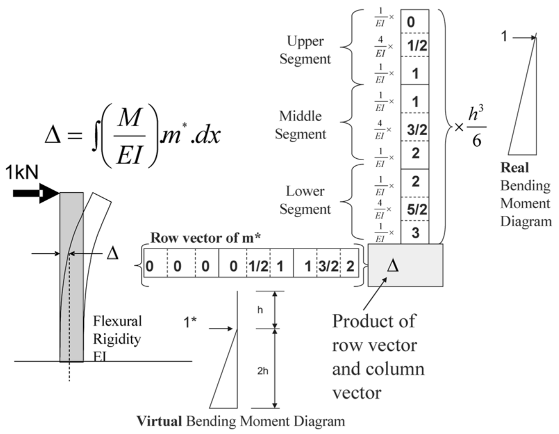


(b) Calculation of deflection by vector multiplication

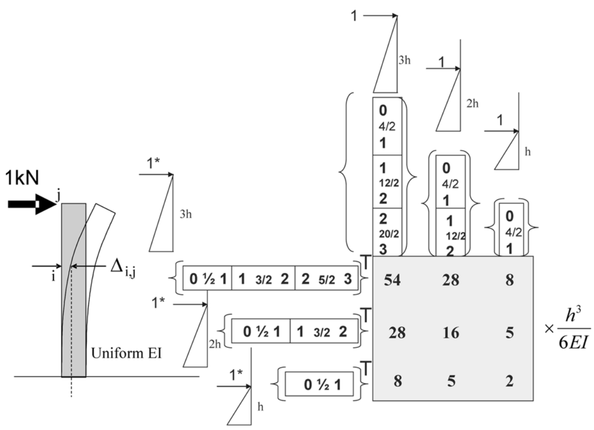


(c) Entries to flexibility matrix by vector multiplications

Fig. 18 Flexibility matrix assemblage for bending of structural wall shear modulus and $A$ is the shear area (or equivalent shear area). Whilst vectors and matrices used in the above illustrations were of the (modest) dimension of 3 degrees of freedom, spreadsheets for vectors, and matrices, of dimension equal to 10 have been developed by the authors for analysis of taller buildings. It is noted that in practice, every two or three stories in the building can be lumped together into a *DOF*. Thus, a macro model of 10 *DOF* (which is characterised by vectors and matrices of dimension equal to 10) can be used to model the dynamic drift behaviour of a building which has 20 or 30 stories.

The *spreadsheet* developed by the authors was used to operate on the *macro* model of a 10-storey, 30 m tall, building which is supported by a dual system of wall-frame as shown below in Fig. 19(a). The structural wall which has a maximum flexural rigidity ($EI$) of 100,000 MN/m$^2$ is assumed to deflect purely in bending (i.e., shear deformation is ignored). The value of $EI$ is curtailed by 50% in the upper half of the building. The equivalent shear rigidity of the moment frame ($GA$) is 1000 MN in the lower half of the building and is reduced by 50% in the upper half of the building. Push-pull actions of the columns in the moment-frame have also been ignored and hence the deflection is purely due to the flexing of the columns in between the floors. The seismic mass on each floor is taken as 150 tonnes. It is shown by modal analysis (as illustrated in Section 3) that the natural periods of the building in the first 3 significant modes of vibration are 0.72 s, 0.19 s and 0.08 s respectively (as shown in Fig. 19(b) in which the mode shapes are also shown). Results of the modal analysis can be used for simulating time-histories for the storey deflections and inter-storey drift demands, in the same manner as that illustrated in Section 3.

A dynamic modal analysis of a finite element model of the same building was performed using the commercial package *SPACEGASS* to verify the accuracy of the developed *spreadsheets*. Results are presented in Fig. 20 for comparison with that presented in Fig. 19.

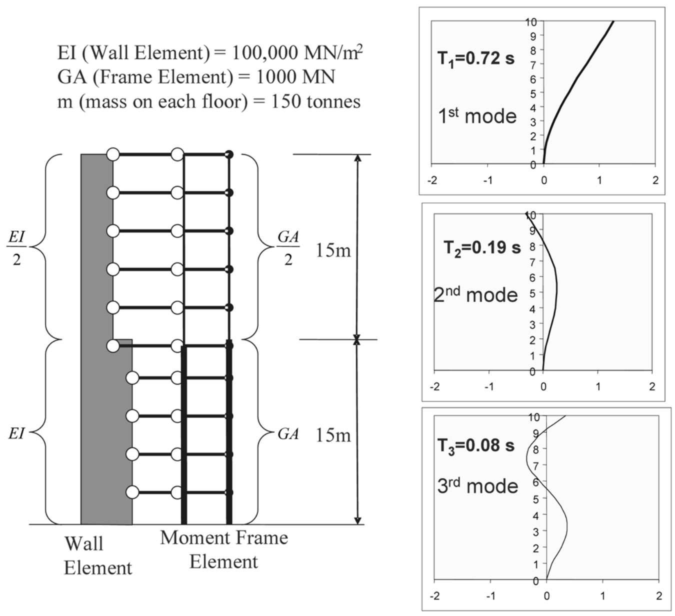


(a) Model (b) Natural period and mode shapes

Fig. 19 Macro model of 10-storey building and modal analysis results

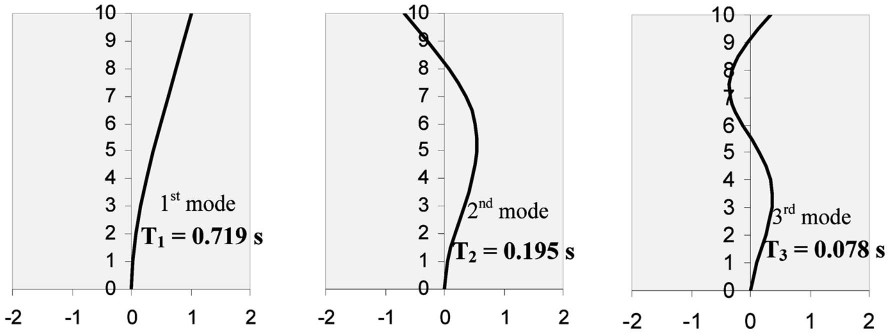


Fig. 20 Modal analysis results from *SPACEGASS*

## 5. Conclusions

This paper illustrates the use of spreadsheets and macro models of single-storey and multi-storey buildings for performing dynamic modal analyses and simulations of the time-histories of the building responses. Modal analysis was accomplished using *Mode Shape Iteration Method* and *Time-history Simulations* were accomplished using *Central Difference Method.* Both methods are very suited to implementation in the spreadsheet environment as demonstrated by worked examples. The simulations enabled maximum inter-storey drift values and the corresponding storey shear forces to be identified. An innovative procedure for constructing the flexibility matrix, stiffness matrix and dynamic matrix of tall buildings has been introduced. The spreadsheet program developed has the capability of analysing buildings that are supported by dual systems of structural walls combined with moment-frames. Variations in the sectional properties of the lateral resisting elements up the height of the building can also be incorporated into the calculations. The operation of the spreadsheet has been demonstrated by the dynamic modal analysis of a 10-storey building which is supported by a dual system of a wall-frame. The accuracy of the calculations by spreadsheets has been verified by comparison with results obtained from the finite element analysis of the same building using a commercial package.

## References

AS1170.4 (2007), *Structural Design Actions. Part 4: Earthquake Actions in Australia*, Standards Australia, Sydney, NSW.

Al Abadi, H., Lam, N.T.K., Gad, E. and Chandler, A.M. (2004), "Earthquake floor spectra for unrestrained building components", *Int. J. Struct. Stab. Dy.,* **4**(3), 361-377.

Al Abadi, H., Lam, N.T.K. and Gad, E. (2006), "A simple displacement based model for predicting seismically induced overturning", *J. Earthq. Eng.,* **10**(6), 775-814.

Chandler, A.M., Lam, N.T.K. and Sheikh, N. (2002), "Response spectrum predictions for potential near-field and far-field earthquakes affecting Hong Kong: soil sites", *Soil Dyn. Earthq. Eng*., **22**, 419-440.

Chopra, A.K. (2000), *Dynamics of Structures – Theories and Applications to Earthquake Engineering* (2nd edition), Prentice Hall, Englewood Cliffs, NJ.

Cotsovos, D.M. and Pavolovic, M.N. (2006), "Simplified FE model for RC structures under earthquakes", *Proceed. Instit. Civil Eng., Struct. Build.,* **159**(2), 87-102.

Elghazouli, A.Y. (2003), "Seismic design procedures for concentrically braced frames", *Proceed. Instit. Civil*

*Eng., Struct. Build.,* **156**(4), 381-394.
Gülkan, P. and Akkar, S. (2002), "A simple replacement for the drift spectrum", *Eng. Struct*., **24**(11), 1477-1484.
Iwan, W.D. (1997), "Drift spectrum: Measure of demand for earthquake ground motions", *J. Struct. Eng-ASCE*, **123**(4), 397-404.
Ju, Y.K. (2006), "Simplified dynamic inelastic analysis of tall buildings", *Proceed. Instit. Civil Eng., Struct. Build.,* **159**(3), 165-178.
Kelly, T. (2004), "Non-linear analysis of reinforced concrete shear wall structures", *Bull. N.Z. Nat. Soc. Earthq. Eng.,* **37**(4), 156-180.
Krawinkler, H. (1996), "Earthquake design and performance of steel structures", *Bull. N.Z. Nat. Soc. Earthq. Eng.,* **29**(4), 229-241.
Lam, N.T.K., Gaull, B.A. and Wilson, J.L. (2007), "Calculation for earthquake loading on building structures in Australia", *Electron. J. Struct. Eng*., Special Issue: Loading on Structures, 22-40.
Lam, N.T.K., Griffith, M.C., Wilson, J.L. and Doherty, K. (2003), "Time history analysis of URM walls in out-of-plane flexure", *J. Eng. Struct.,* **25**(6), 743-754.
Lam, N.T.K., Wilson, J.L. and Hutchinson, G.L. (2000), "Generation of synthetic earthquake accelerograms using seismological modelling : A review", *J. Earthq. Eng*., **4**(3), 321-354.
Lam, N.T.K., Wilson, J.L. and Hutchinson, G.L. (1995), "The seismic resistance of unreinforced masonry cantilever walls in low seismicity areas", *Bull. N.Z. Nat. Soc. Earthq. Eng.,* **28**(3), 179-195.
Lam, N.T.K., Wilson, J.L. and Chandler, A.M. (2001), "Seismic displacement response spectrum estimated from the frame analogy soil amplification model", *J. Eng. Struct.*, **23**, 1437-1452.
Miranda, E. (1999), "Approximate seismic lateral deformation demands in multistory buildings", *J. Struct. Eng-ASCE*, **125**(4), 417-425.
Miranda, E. and Reyes, C.J. (2002), "Approximate lateral drift demands in multi-story buildings with non-uniform stiffness", *J. Struct. Eng-ASCE*, **128**(7), 840-849.
Miranda, E. and Akkar, S.D. (2006), "Generalized interstory drift spectrum", *J. Struct. Eng-ASCE,* **132**(6), 840-852.
Miranda, E. and Ruiz-Garcia, J. (2002), "Evaluation of approximate method to estimate maximum inelastic displacement demands", *J. Earthq. Eng. Struct. D.,* **31**, 539-560.
Numayr, K.S., Al-Jallamdeh, S.A. and Al-Akhras, N.M. (2003), "Dynamic stiffness of reinforced concrete beams", *Proceed. Instit. Civil Eng., Struct. Build.,* **156**(4), 373-380.
Paulay, T. and Priestley, M.J.N. (1992), *Seismic Design of Reinforced Concrete and Masonry Buildings*, John Wiley & Sons, Inc.
Priestley, M.J.N. (1996), "Displacement-based seismic assessment of existing reinforced concrete buildings", *Bull. N.Z. Nat. Soc. Earthq. Eng.,* **29**(4), 256-272.
Priestley, M.J.N. (1998), "Brief comments on elastic flexibility of reinforced concrete frames and significance to seismic design", *Bull. N.Z. Nat. Soc. Earthq. Eng.,* **31**(4), 246-259.
Priestley, M.J.N. and Kowalsky, N.J. (1998), "Aspects of drift and ductility capacity of rectangular cantilever structural walls", *Bull. N.Z. Nat. Soc. Earthq. Eng.,* **31**(2), 73-85.
Priestley, M.J.N., Calvi, G.M. and Kowalsky, M.J. (2007), *Displacement-Based Seismic Design of Structures,* IUSS PRESS, Pavia, Italy.
Qian, J. and Chen, Q. (2005), "A macro model of shear walls for push-over analysis", *Proceed. Instit. Civil Eng., Struct. Build.,* **158**(2), 119-132.
Yun, H.D., Choi, C.S. and Lee, L.H. (2004), "Behaviour of high-strength concrete flexural walls", *Proceed. Instit. Civil Eng., Struct. Build.,* **157**(2), 137-148.